Int. J. Advanced Design and Manufacturing Technology, 2023, Vol. 16, No. 2, pp. 91-102

DOI: 10.30486/admt.2023.1959673.1352 ISSN: 2252-0406 https://admt.isfahan.iau.ir

Study on the Thermophysical Properties of Hybrid Nanofluid Based on Aircraft De/Anti-Icing Fluid at Low Temperatures

Nasim Nayebpashaee
Department of Metallurgy and Mechanical Engineering,Technology and Engineering Research Center, Standard Research Institute (SRI), Karaj, Iran
E-mail: n.nayebpashaee@standard.ac.ir

Received: 26 May 2022, Revised: 17 September 2022, Accepted: 17 September 2022

Abstract: This work involves an experimental study of the thermophysical properties of hybrid nanofluids of TiO_2 and graphene in a binary mixture of water and ethylene glycol. Hybrid nanofluid samples with different volume fractions (0.05-2.5%) were prepared by dispersing equal volumes of TiO_2 and graphene nanoparticles in a binary mixture of water and ethylene glycol in the ratio of 50-50% by volume. The thermal conductivity, surface tension, and dynamic viscosity of the hybrid nanofluids were measured at temperatures ranging from 253 K to 303 K. The experimental results showed that the low concentration samples exhibited shear thinning non-Newtonian behavior, while the high concentration samples exhibited shear thickening non-Newtonian behavior. The measurements showed that the thermal conductivity of the nanofluids increases by up to 41.93% with increasing nanoparticle concentration and temperature. The surface tension improves by 43.61%, 39.77%, and 51.98% at concentrations of 2.5%, 2%, and 2% by volume at temperatures of 258.15 K, 268.15 K, and 283.15 K, respectively. In terms of aircraft deicing fluid performance, the addition of TiO2 and graphene nanoparticles at less than 0.5% by volume contributes to the improvement of aircraft deicing fluid performance.

Keywords: Aircraft De/Anti-Icing Fluid, Concentration Effect, Dynamic Viscosity, Hybrid Nanofluids, Low Temperatures, Thermal Conductivity

Biographical notes: Nasim Nayebpashaee is Assistant Professor at the Department of Metallurgy and Mechanical Engineering, Technology and Engineering Research Center, Standard Research Institute (SRI), Karaj, Iran. She received her MSc and PhD in Materials and Metallurgy Engineering from Iran University of Science and Technology (IUST), Tehran, Iran, in 2011 and 2017. Her current research interest includes Surface engineering, Hybrid Nano fluids and RTV insulator coatings.

Research paper

1 INTRODUCTION

Nanofluid is a colloidal suspension consisting of nanoparticles and a base fluid [1-2]. Previous research has revealed that nanofluids have superior thermophysical properties such as thermal conductivity, thermal diffusivity, viscosity, and convective heat transfer coefficients compared to base fluids such as oil or water [3-4]. Hybrid nanofluids are the next generation of nanofluids that consist of a combination of more than one type of nanoparticles suspended in a base fluid [2], [5]. The thermophysical and rheological properties of hybrid nanofluids, such as thermal conductivity and viscosity, are higher than those of single nanofluids [2], [4-7] which recommend that hybrid nanofluids have great potential for thermodynamic applications [8-9]. Aircraft ground de/anti-icing is a treatment that removes ice and semi-frozen moistuire and protects the aircraft surfaces from the formation of these until takeoff. Deicing fluid is generally heated and sprayed under pressure to remove ice and snow on the aircraft.There are four standard types of aircraft deicing fluids: type I, II, III, and IV [10-13]. Typical aircraft deicing fluids are non-Newtonian pseudoplastic fluids containing freezing point depressants, surfactants, corrosion inhibitors, thickeners, defoamers, pH modifiers, dyes, oils, antioxidants, and antimicrobials [12], [14-15]. Thickening agents impart shear thinning rheological behavior to anti-icing fluids. When the aircraft is stationary, the viscosity of the fluid is very high. When the aircraft accelerates for takeoff, the shear of the fluid increases, resulting in a drastic decrease in viscosity and allowing the fluid to easily detach from the aircraft surfaces [12], [15].

Recently, the properties of nanofluids have been extensively studied [16-21]. There are many experimental studies to investigate the thermal conductivity and viscosity behavior of nanofluids with different nanoparticles [6], [22-28]. These researches will lead to the development of nanofluids for various industrial applications. Most of these investigations have been performed at intermediate and high temperatures (temperatures between 296 K and 328 K). Very few studies have specifically focused on the rheological behavior and thermophysical properties of nanofluids at intermediate and low temperatures [29]. The lack of such studies in the field of the behavior of hybrid nanofluids at subzero temperatures is even more evident and prevents the identification of application areas in appropriate industrial applications [29]. One of the potential applications for nanofluids at low temperatures is aircraft de/anti-icing fluid which has not been considered yet.

Recently, only a few research works have focused on the rheological behavior of hybrid nanofluids. The thermophysical and rheological properties of hybrid nanofluids are rarely studied at low temperatures and especially sub-zero temperatures. The lack of measurements of thermophysical properties of hybrid nanofluids at low temperatures is the main motivation for this research. Moreover, according to the present author's consideration, there have been no studies on the thermophysical and rheological behavior of nanofluids based on aircraft de/anti-icing fluid. Accordingly, in the present study, the effect of nanoparticle concentration and temperature on the thermophysical properties and rheological behavior of TiO_2-geraphene: aircraft de/anti-icing-water hybrid nanofluid was experimentally investigated. For this purpose, nanofluid samples with different solid volume fractions were prepared and investigated at different temperatures and shear rates. The hybrid nanofluids are currently prepared using water- aircraft de/anti-icing fluid mixture (50:50 by volume at 298.15 K) and sodium dodecyl sulfonate (SDS) and oleic acid (OA) as surfactants. Different concentrations of nanoparticles were considered, such as 0.05, 0.1, 0.5, 1, 1.5, 2 and 2.5. vol. %, respectively. Also, the hybrid nanofluid properties were experimentally investigated in the temperature range of 253.15 to 293.15 K to verify the performance of such hybrid nanofluids in cold condition and to demonstrate their potential applications.

2 MATERIALS AND METHODS

The TiO_2 nanoparticles and graphene nanoplatelets used in this study were obtained from US research nanomaterials (USA) with the properties tabulated in "Tables 1 and 2". The aircraft de/anti-icing fluid was "Kilfrost ABC -3", which is identified as aircraft de /anti-icing fluid AMS1428 (ISO11078) [30] Type II. The physicochemical properties of aircraft de/anti-icing fluid are listed in "Table 3".

Table 1 Specifications of TiO_2 nanoparticles used in this study

Parameter	Value
Purity	99+%
Color	white
Size	21 nm
Morphology	nearly spherical
Specific surface area (SSA)	220 m^2/g
Density	3900 kg/m^3

Table 2 Specifications of graphene nanoplatelets used in this study

Parameter	Value
Purity	99.5%
Color	black
Thickness	2-18 nm
Morphology	plate-like
Specific surface area (SSA)	500-1200 m^2/g
Density	230 kg/m^3

Table 3 Characteristics of aircraft de/anti-icing fluid [31]

Characteristic	Value
Appearance	Clear, colorless liquid
Odor	Odorless
Density	1.040 g/mol
Boiling point	104 °C
Viscosity	4900 mPa.s (@20 °C)

The XRD studies were carried out by a Philips PW1730 X-ray diffractometer using Cu (Kα =1.54060 A°) radiation for 2θ (20° to 80°) in steps of 0.03° with step scan time 0.6s. The test was performed to identify the phase and crystal structure of nanoparticles.

To be able to investigate the surface morphology of the nanoparticles, TESCANMIRA3 Scanning Electron Microscopy (SEM) was used.

The size and morphology of nanoparticles were analyzed by Transmission Electron Microscopy (TEM) using Philips CM120 instrument.

Brunauer-Emmett-Teller (BET, BELSORB MINI II, BEL, JAPAN) N_2 adsorption at 77 K was performed to determine the molecular sieve area, porosity, and specific surface area (SSA) of TiO_2 nanoparticles and geraphene nanoplatelets using a five-point isotherm BET ((TriStar II Plus, Micrometrics) after degassing the samples for ≥1 h at 140 °C). The BET Equation was used to calculate the specific surface area.

In the present study, the hybrid nanofluids were prepared using a two-step method. The base fluid was a combination of distilled water and aircraft de/anti-icing fluid (50:50 concentrations in volume percent) and the amount of 0.2 volume percent oleic acid (OA) and 0.2 weight percent sodium dodecyl sulfonate (SDS) as surfactants to stabilize and disperse the nanoparticles. The properties of oleic acid are listed in "Table 4".

Table 4 Characteristics of oleic acid [29], [32-33]

Characteristic	Value
Chemical formula	$C_{18}H_{34}O_2$
Appearance	Clear, Pale yellow
Viscosity(@293.15K)	38.80 mPa.s
Melting point	286.15 K
Freezing point	277.15 K
Cloud point (CP)	283.15 K±1
Pour point (PP)	273.15 K±1

The nanoparticles were dispersed in the base fluid with solid volume fractions of 0.05, 0.1, 0.5, 1, 1.5, 2 and 2.5%. Equal amounts of TiO_2 nanoparticles and graphene nanoplatelets were dispersed in the base fluid. The required amounts of TiO_2 and graphene nanoparticles for the preparation of the hybrid nanofluid samples were determined using Equation (1):

$$\varphi = \frac{\left(\frac{w}{\rho}\right)_{TiO_2} + \left(\frac{w}{\rho}\right)_{graphene}}{\left(\frac{w}{\rho}\right)_{TiO_2} + \left(\frac{w}{\rho}\right)_{graphene} + \left(\frac{w}{\rho}\right)_{water} + \left(\frac{w}{\rho}\right)_{De/Anti-icingfluid}} \times 100 \quad (1)$$

Where, φ is the nanoparticle volume fraction percentage, ρ is the density in kg/m3 and W is the mass in kg. The masses of the nanoparticles, aircraft de/anti-icing fluid and water used to prepare a volume of 400 ml of the hybrid nanofluid were calculated and listed in "Table 5".

Table 5 Mass of nanoparticles, ethylene glycol (EG) and water used for preparing a volume of 400 ml of hybrid nanofluid

Solid volume fraction (%)	Mass [±0.001] (g)			
	TiO_2	G	Aircraft de/anti-icing fluid	Water
0	0.000	0.000	199.642	222.640
0.05	0.390	0.023	199.542	222.529
0.1	0.780	0.046	199.442	222.417
0.5	3.990	0.230	198.644	221.527
1	7.810	0.460	197.646	220.414
1.5	11.770	0.690	196.647	219.300
2	15.660	0.920	195.649	218.187
2.5	19.550	1.150	194.651	217.074

The concentrations of surfactants were constant for all samples. The nanoparticles were weighed using a high precision weighing balance. A magnetic stirrer (IKA, model RCT basic) was used for 3 hours to prepare the stable samples. To separate the agglomerations, the nanoparticles were then dispersed in the base fluid by continuous ultrasonic sonication for 4 hours. The ultrasonic processor used in this study (Hielscher Company, Germany) has a wattage of 150 W and a frequency of 20 kHz. The ultrasound processor was set to operate in pulse mode (10 s on and 10 s off) and with an amplitude of 90%. The duration of the ultrasound was set to one hour.

Zeta potential measurement was used as the method to evaluate the stability of nanofluids. The zeta potential of the hybrid nanofluids was measured at 298.15 K using a Zetasizer Nano ZS90 from Malvern, Britain.

The viscosity of TiO_2 - graphene/ aircraft de/anti-icing fluid -water nanofluids with solid volume fractions of 0.05% to 2.5% was measured in a temperature range of 263.15 K to 303.15 K. A Brookfield viscometer with a

temperature bath (supplied by Brookfield Engineering Laboratories) was used to measure the viscosities of TiO_2 - graphene/ aircraft de/anti-icing-water nanofluids in the shear rate range of 0.3 RPM – 70 RPM. The ranges of repeatability and accuracy of the viscometer are, respectively, ±0.2% and ±1.0%. The viscometer was tested with a mixture of pure water and ethylene glycol (50:50) at various temperatures before being used to measure the dynamic viscosity of the hybrid nanofluids, and reasonable agreement was obtained between the measured data and the data reported in the ASHRAE handbook [34]. As shown in "Fig. 1(a)", the absolute average deviation between the ASHRAE data [34] and the experimental data in this study was less than 2%.

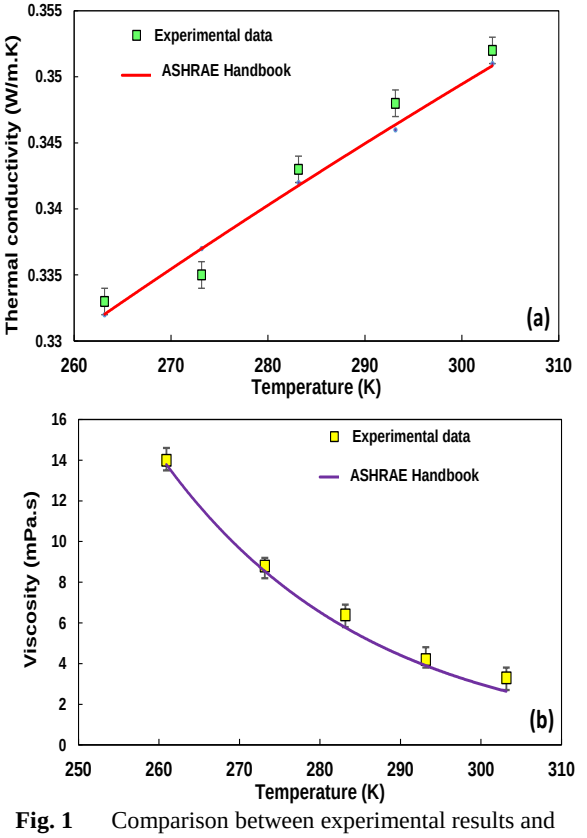

Fig. 1 Comparison between experimental results and ASHRAE data [34] on: (a): viscosity, and (b): thermal conductivity of a mixture of water-ethylene glycol (50–50) at different temperatures.

The thermal conductivity of the nanofluid was estimated using a thermal analyzer (Decagon Devices, Inc., model KD2 Pro). The accuracy of the sensor was ±5% over the temperature range of 273.15 to 303.15 K. To ensure the accuracy of the KD2 Pro instrument, prior to measuring the thermal conductivity of the hybrid nanofluids, the thermal conductivity of water-ethylene glycol mixtures containing 50-50 recorded with the KD2 Pro at various temperatures was compared with the data from the ASHRAE handbook [34]. As can be seen in "Fig. 1 (b)", the experimentally determined thermal conductivity of the base fluid agrees well with the available data, with a small deviation (<0.5%) in the mentioned temperature range.

In the present study, the surface tension of the nanofluids was measured using the Surf-S1 device. The device was first calibrated by measuring the surface tension of acetone at 298.15 K. The surface tension of the prepared hybrid nanofluids was then measured at different constant temperatures ranging from 258.15 K to 283.15 K. Each value reported is the average of three measurements with an uncertainty of 0.1 mN m^{-1}.

3 RESULT AND DISCUSSION

The XRD patterns of TiO_2 nanoparticles and graphene nanoplatelets are shown in "Fig. 2".

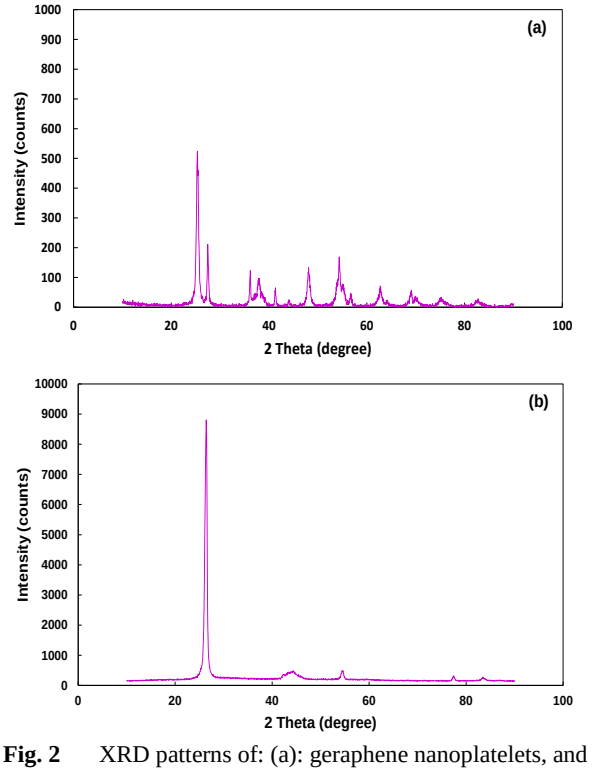

Fig. 2 XRD patterns of: (a): geraphene nanoplatelets, and (b): nanoscale TiO_2.

As shown in "Fig. 2(a)", the XRD outputs of graphene nanoplatelets reveal a sharp and tight peak at 26.455° and some short peaks at 43.348°, 54.484°, 77.421°, and 83.478°; the strong peak at 2θ = 26.455° with a d-spacing of 3.370 Å is attributed to the (002) crystal plane [35-36].

As can be seen in "Fig. 2(b)", diffraction peaks of nanosized TiO_2 are shown at 25.334°, 27.451°, 36.177°, 38.049°, 41.237°, 48.010°, 54.305°, 60.871°, and 69.206°. No peaks of impurities were observed.

Nanoparticle characterization was performed using TEM images. Figure 3 (a) is a TEM image of graphene nanoplatelets and shows many wrinkles and folded regions, which are a characteristic structure of graphene nanosheets. The TEM images of TiO_2 nanoparticles are shown in "Fig. 3 (b)". Virtually all particles showed a quasi-spherical shape.

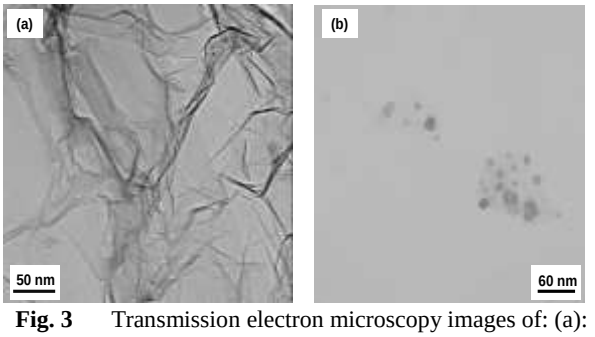

Fig. 3 Transmission electron microscopy images of: (a): Graphene nanoplatelets, and (b): TiO_2 nanoparticles.

The hydrophobicity of nanoparticles depends on their surface area. The active surface area of nanoparticles was determined using BET analysis. The BET surface area, pore volume, and average pore size of graphene nanoplatelets were determined to be 27.51 m²/g, 0.089 cm³/g, and 129.00 Å, respectively. The 5 N2 adsorption/desorption isotherms and pore diameter distribution of of nanoparticles are shown in "Figs. 4 and 5".

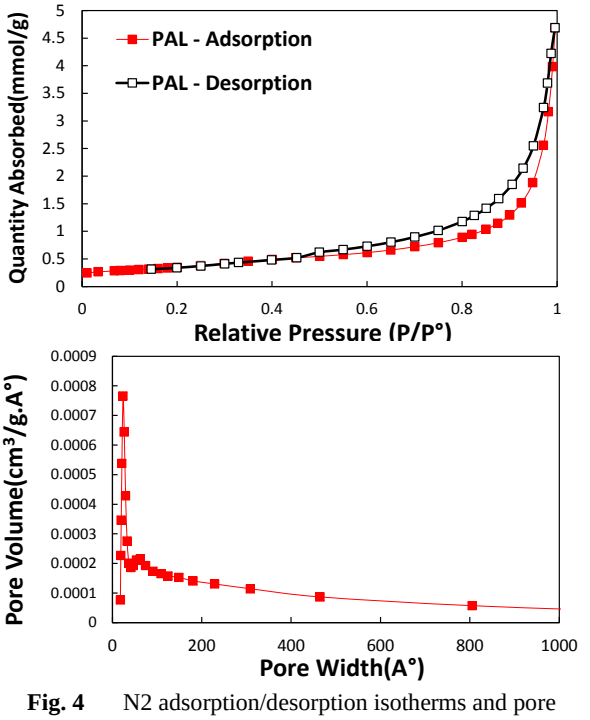

Fig. 4 N2 adsorption/desorption isotherms and pore diameter distribution of Graphene nanoplatelets.

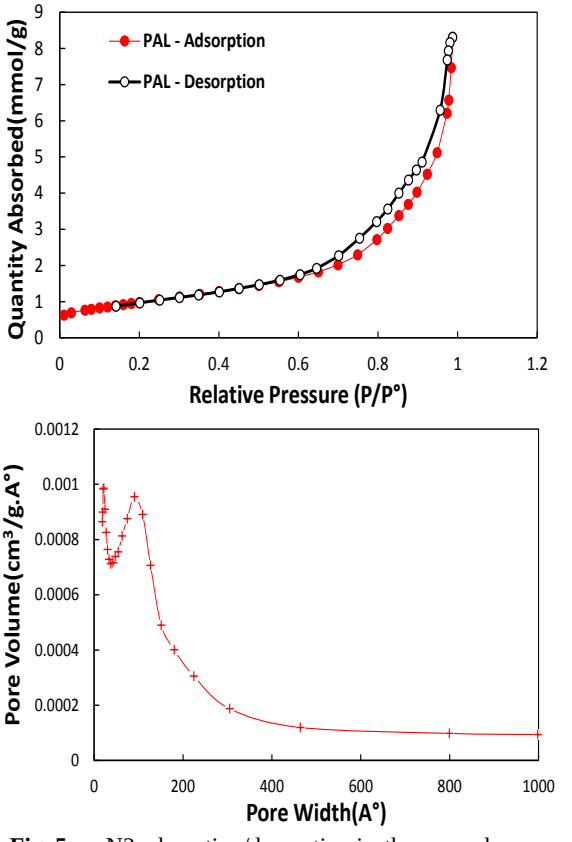

Fig. 5 N2 adsorption/desorption isotherms and pore diameter distribution of TiO_2 nanoparticles.

Particle size, pore structure and surface area of the nanoparticles were characterized using BET analysis. The adsorption-desorption isotherm (Figs. 4 and 5) shows a hysteresis loop very similar to the IV type isotherm. The BET surface area, pore volume, and average pore size of TiO_2 nanoparticles were determined to be 178.15 m²/g, 0.78 cm³/g, and 174.58 Å, respectively. The relationship between specific surface area and particle size in the BET model is ("Eq. (2)"):

$$d_{BET} = \frac{6000}{\rho\, S_{BET}} \qquad (2)$$

Zeta potential analysis was performed to confirm the stability of the hybrid nanofluids. The zeta potential of the hybrid nanofluids at 298.15 K as a function of solid volume fraction and standing time is plotted in "Fig. 6". As can be seen in "Fig. 6", the zeta potential values of the hybrid nanofluids ranged from -29 to -59, which is sufficient for a stable suspension [37-39]. It can be seen that the addition of surfactants increases the stability of the nanofluids.

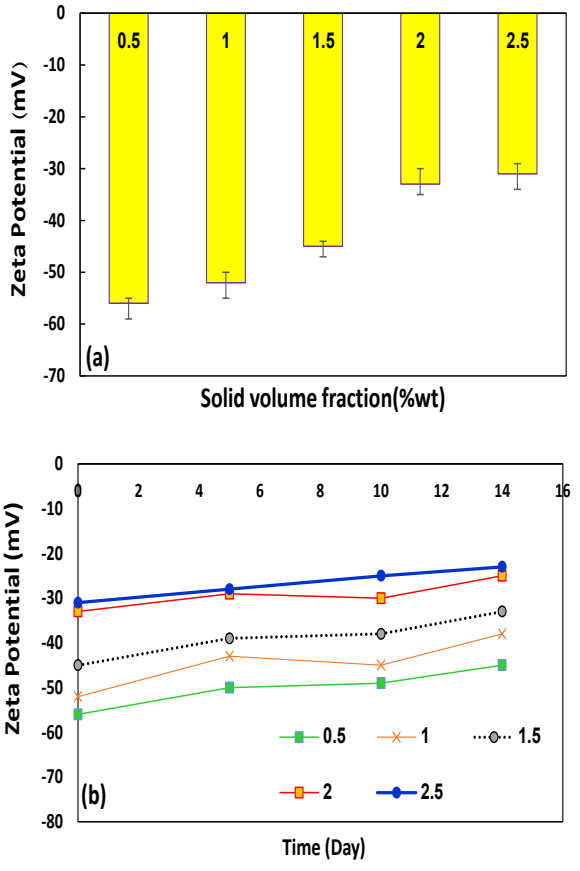

Fig. 6 Zeta potential of hybrid nanofluids: (a): at different concentrations, and (b): with standing time.

As shown in "Fig. 6 (b)", aggregation of nanoparticles deteriorates the dispersion stability of the nanofluid with increasing the standing time. The maximum values of zeta potential were associated with higher concentrations of nanoparticles. This could be due to the aggregation of particles at higher concentrations [40-42].

Dynamic viscosity measurements of the hybrid TiO_2-graphene nanoplatelets/aircraft de/anti-icing-water nanofluid were performed in a temperature range of 263.15 K to 293.15 K for different suspensions with volume fractions of 0.05%, 0.1%, 1%, 1.5%, 2%, and 2.5%.

In order to study the viscosity of a hybrid nanofluid, it must first be determined whether it is a Newtonian or a non-Newtonian fluid. Newtonian fluids obey Newton's law of viscosity. The shear stress in these fluids is independent of the shear rate. It is characterized by the following relation: ("Eq. (3)"):

$$\tau = m\dot{\gamma} \tag{3}$$

Where, μ is the apparent viscosity, τ is the shear stress, and $\dot{\gamma}$ is the shear rate. Non-Newtonian fluids contradict Newton's law, and their shear stress varies with shear rate. The following Equation illustrates the non-Newtonian behavior ("Eq. (4)"):

$$\tau = m\dot{\gamma}^{n} \tag{4}$$

Where, n is the power law index and m is the consistency index. When n <is 1, shear thinning is defined. Shear thickening is associated with n > 1.

Figure 7 shows the dynamic viscosity as a function of shear rate at 298 K for various values of solid volume fraction.

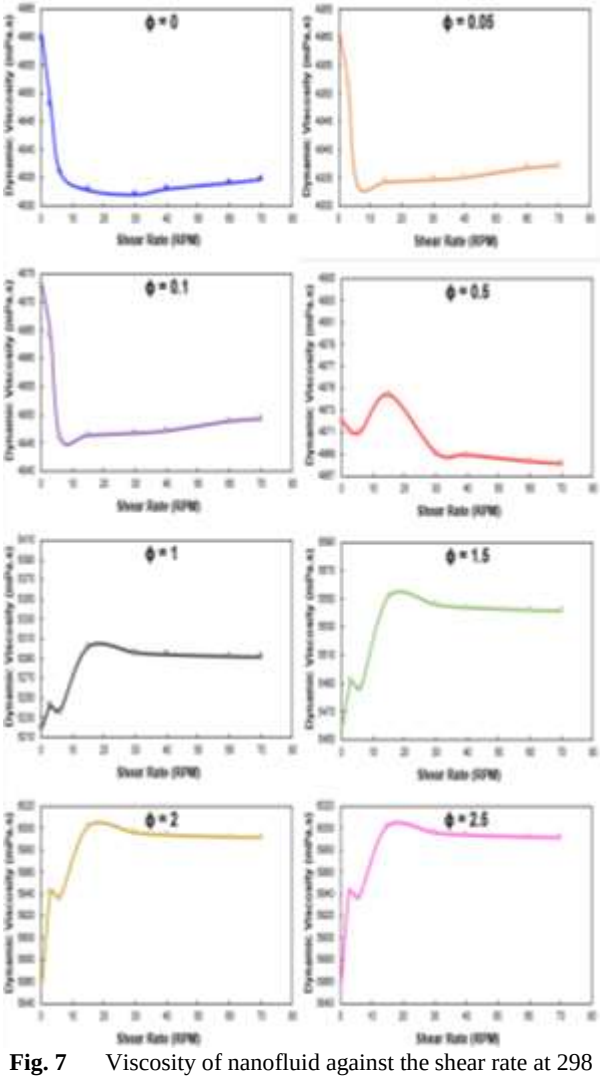

Fig. 7 Viscosity of nanofluid against the shear rate at 298 K for different solid volume fractions.

As can be seen, the shear stress depends on the shear rate for hybrid nanofluids with solid volume fractions between 0.5 and 2.5%. For these samples, an increase in shear rate at constant temperature leads to a nonlinear decrease in viscosity, indicating non-Newtonian

behaviour at all temperatures studied. It can also be observed that the n values are less than 1, indicating that the hybrid nanofluids exhibit shear thinning behaviour at high concentrations. Samples with solid volume fractions of more than 0.5% show a different rheological behavior. For samples with a solid volume fraction in the range of 0.5-2.5%, an increase in shear rate leads to a relative increase in viscosity and the hybrid nanofluid tends to exhibit non-Newtonian shear thickening behavior.

According to AMS 1428 [30], the aircraft deicing fluid type II is pseudoplastic, i.e., it contains a polymeric thickener that prevents it from flowing off the aircraft surface immediately. Aircraft deicing fluid type II remains in place until the aircraft reaches a speed of 100 knots (190 km/h) and the viscosity decreases due to pressure. The fluid used must be removed from the surfaces before takeoff to avoid affecting the aircraft's aerodynamic performance. The addition of nanoparticles with a volume fraction of 0 to 0.5% increases the viscosity and does not change the non-Newtonian (shear thinning) behavior of the base nanofluid, which is the main requirement for the operation of the aircraft deicing fluid type II. At higher concentration, the rheological behavior of the fluid changes. Therefore, the addition of these two types of nanoparticles in volume fractions of less than 0.5% helps to improve the performance of the aircraft deicing fluid. As the volume fraction of solids increases, the number of nanoparticles increases, resulting in more spontaneous nanoparticle motion and collisions with base fluid molecules. In contrast, as the number of nanoparticles increases (i.e., as the concentration of nanoparticles increases), the distance between nanoparticles decreases and the probability of nanoparticle agglomeration increases. An increase in the volume fraction of nanoparticles increases the collisions between particles and the possible agglomeration increases, resulting in an increase in viscosity and consistency index.

Figure 8 shows the dynamic viscosity values as a function of shear rate at different temperatures for different solid volume fractions. For hybrid nanofluids with solid volume fractions of 0.05 and 0.1 vol% at temperatures below the freezing point (T=263.15 K), the shear flow curves show that the viscosity values increase slightly with increasing shear rate, suggesting non-Newtonian behaviour. The surprising behaviour of the nanofluid at temperatures below the freezing point has already been described by some researchers [29], [43]. In the present study, this phenomenon can be attributed to the existence of oleic acid. In this study, oleic acid is added to the base fluid as a surfactant.

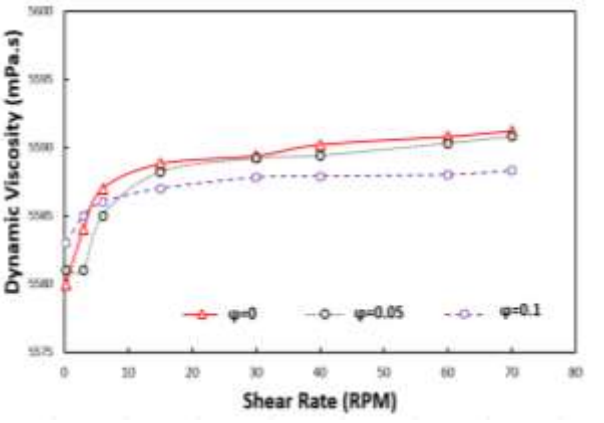

Fig. 8 Dynamic viscosity values versus the shear rate at different temperatures for various solid volume fractions.

The pour point and cloud point are important indicators of the flowability of oleic acid at low temperatures as a nonionic surfactant. As shown in "Table 4", the cloud point of oleic acid is 283.15 K±1, which is the temperature at which the liquid begins to cloud due to crystallisation under organised cooling [32]. The cloud point shows that the surfactants tend to exist as solid particles in the base liquid. Oleic acid is no longer completely soluble in the base fluid at temperatures below the cloud point, resulting in a cloudy texture. The pour point of oleic acid is 273.15 K±1, which is the temperature at which the flow properties change [32]. At temperatures below the freezing point, oleic acid tends to self-aggregate and form macrocrystalline structures that restrict the easy flow of the system and increase the internal friction, which in turn increases the viscosity [29]. Moreover, the improvement in viscosity at sub-freezing temperatures could be due to graphene nanoplatelets, due to their unique structures and inherent properties. The precipitation of oleic acid as the second phase allowed the graphene nanoplatelets to agglomerate and form hydroclusters [44].

Banisharif et al.[29] investigated the thermophysical properties of Fe_3O_4 nanofluids based on water- ethylene glycol mixture and reported Newtonian behaviour at 0.01%-0.1% solid concentration in the temperature range of 263.15 K - 293.15 K and non-Newtonian behaviour at 253.15 K. A similar trend was observed by Kulkarni et al. [43] using CuO nanoparticle based nanofluids in 40:60 water/ethylene glycol mixture. According to this study [43], the nanofluid exhibits Newtonian behaviour in the temperature range of 238.15 - 323.15 K and the viscosity of the nanofluid decreases with shear rate at 253.15 K, indicating shear thinning behaviour.

Temperature is the most important and influential parameter for viscosity. As can be seen in "Fig. 9", the viscosity of the hybrid nanofluid decreases with increasing temperature.

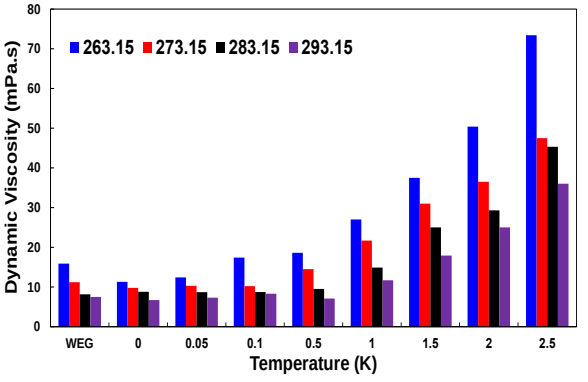

Fig. 9 Experimental values of viscosity for various volume concentrations of nanofluids with respect to temperature.

This is due to the fact that the intermolecular attraction between the nanoparticles and their base fluids decreases with increasing temperature. Most literature reports [22], [45] found a downward trend in viscosity with increasing temperature. However, some authors [50] found that increasing the temperature had no effect on the relative viscosity. Zhao et al [46] studied the viscosity of alumina-water nanofluids with different volume fractions of 1.31%, 2.72%, 4.25% and 5.92% at different temperatures between 296 and 313 K and reported that the viscosity strongly depends on the volume fraction of Al_2O_3 nanoparticles and remains constant with a change in temperature. Chen et al [47] found no difference in relative viscosity with increasing temperature in their studies on TiO_2 ethylene glycol nanofluid in the temperature range of 293-333 K.

Based on the results of measuring the dynamic viscosity of graphene TiO_2 / aircraft de / anti-ice fluid - water hybrid nanofluid, the addition of nanoparticles in the volume fraction ranges from 0 to 0.5%, in addition to increasing the viscosity, shows non-Newtonian behavior shear-thining nanofluid the base, which is the main condition for the performance of aircraft de / anti-ice fluid. Therefore, the addition of these two types of nanoparticles in volume fractions of less than 0.5% helps to improve the performance of aircraft de / anti-icing fluid.

In this study, the thermal conductivity measurements of hybrid nanofluids of graphene-TiO_2/ aircraft de/anti-icing fluid - water hybrid nanofluid were carried out in a temperature range of 263.15 to 303.15 K for suspensions with solid volume fraction of 0.05, 0.1, 0.5, 1.0, 1.5, 2.0, and 2.5%. The effects of temperature and solid volume fraction on the thermal conductivity of the hybrid nanofluid were investigated.

Figure 10 shows the thermal conductivity of hybrid nanofluids of graphene, TiO_2, aircraft depots and anti-icing agents, and water as a function of the volume fraction of the solid at different temperatures.

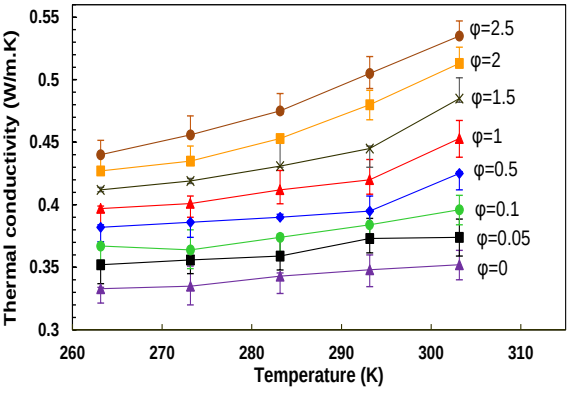

Fig. 10 The effect of volume fraction of nano-particles on thermal conductivity at different temperatures.

As can be seen in this figure, the thermal conductivity of the hybrid nanofluid increases with the volume fraction of the nanoparticles. Assuming a uniform suspension, the number of particles in a given volume of the hybrid nanofluid is high and the distance between the solid particles in the base fluid is relatively smaller than at low concentrations. The kinetic energy of the particles increases with increasing temperature, as does the number of random collisions between the particles. The increased collisions between the nanoparticles increase the energy exchange between the particles. This increases the thermal conductivity of the base fluid. This improvement is even more impressive for hybrid nanofluids with high concentrations. At low concentrations, the large distance between the particles prevents a significant improvement in thermal conductivity.

Figure 11 shows the changes in the ratio of the thermal conductivity of the hybrid nanofluid to the base fluid as a function of temperature and solid volume fraction.

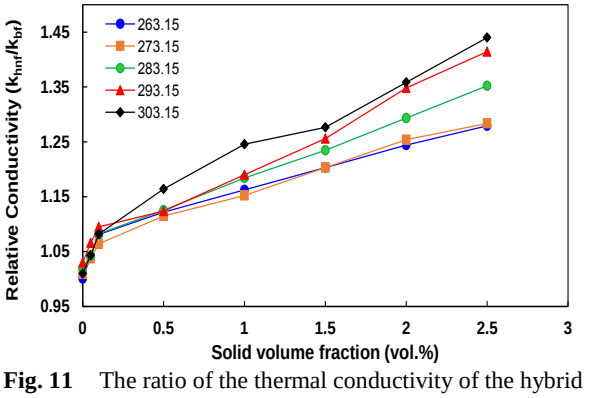

Fig. 11 The ratio of the thermal conductivity of the hybrid nanofluid to the base fluid in terms of solid volume fraction at different temperatures.

It can be observed that the ratio of thermal conductivity of the hybrid nanofluids increases with increasing temperature and increasing solid volume fraction. The thermal conductivity increases with increasing

concentration of nanoparticles, but on the other hand, agglomeration of nanoparticles may occur. The agglomeration of nanoparticles decreases the surface area to volume ratio and results in lower thermal conductivity. The results show that the thermal conductivity of hybrid nanofluids increases with increasing temperature. As shown in "Fig. 11", the effect of temperature on the thermal conductivity of hybrid nanofluids is more remarkable at higher solid volume fractions (1-2.5%). Brownian motion and collisions between nanoparticles are the fundamentals of thermal conductivity. At high concentrations, the influence of temperature becomes more evident. The improvement of thermal conductivity increases with the volume fraction of nanoparticles. The dispersion and stability of nanoparticles in the base fluid are the essential conditions for the efficient use of Nanofluids in many applications [48]. As can be seen in this figure, the thermal conductivity ratio increases by about 41.93% and 3.95% for the highest volume fraction, 2.5% by volume, at the maximum and minimum test temperatures, respectively.

The results are consistent with the results of other studies. The studies show that thermal conductivity is strongly dependent on temperature, particle size, volumetric concentration of particles, particle properties and base fluid properties [2], [4], [23] .

The results of thermal conductivity of graphene- TiO_2/ aircraft de/anti-icing fluid - water hybrid nanofluid show that the thermal conductivity properties and thus the efficiency of aircraft de/anti-icing fluid are improved by the addition of nanoparticles.

Surface tension is the force acting per unit length of the surface of a liquid perpendicular to the force. Surface tension is a critical factor in the application of hybrid nanofluids.

The surface tension of the hybrid nanofluid composed of TiO_2-graphene nanosheet/ aircraft de/anti-icing fluid - water was measured for different suspensions with volume fractions of 0.05%, 0.1%, 1%, 1.5%, 2% and 2.5% at temperatures ranging from 253.15 K to 283.15 K.

Figure 12 shows the change in surface tension as a function of temperature and volume fraction of solid. In "Fig. 12", it can be seen that the surface tension increases with the addition of nanoparticles to the base fluid. The addition of nanoparticles to the base fluid causes an interaction between the molecules of the nanoparticles and the base fluid. As a result, the forces of the nanoparticles and the neighbouring nanoparticles, as well as the forces of the liquid molecules at the liquid surfaces, overlap. As a result, attractive Van der Waals forces occur, which increase the surface free energy and improve the surface tension [25], [49].

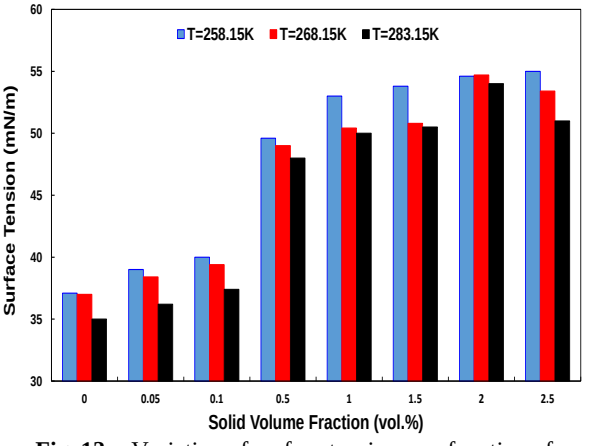

Fig. 12 Variation of surface tension as a function of temperature and solid volume fraction.

The surface tension of hybrid nonfluids decreases with increasing temperature, as shown in "Fig. 12". The thermodynamic motion of the molecules and Brownian motion enhanced by the increase in temperature could be the reason for the decrease in surface tension of nanofluids. Surface tension is determined by intermolecular forces. Intermolecular forces determine surface tension. When the temperature increases, the molecules of the base fluid are more involved and move faster. As a result, the intermolecular forces become weaker and the attraction between the nanoparticles decreases [50].

The surface tension of the hybrid nanofluids increases by nearly 43.61%, 39.77%, and 51.98% at temperatures of 258.15 K, 268.15 K, and 283.15 K, respectively, at concentrations of 2.5%, 2%, and 2% by volume. The molecules of the nanoparticles and the base fluid interact when the nanoparticles are applied to the base fluid. As a result, the forces exerted by the nanoparticles and their neighbors, as well as the forces exerted by the liquid molecules, act on the liquid surfaces. As a result, attractive Van der Waals forces are exerted, which increase the surface free energy and thus the surface tension. The results are also comparable with those of other studies [49], [51].

In terms of aircraft deicing fluid performance, increasing the surface tension of the fluid helps improve its performance in covering aircraft surfaces against precipitation of supercooled raindrops and snow, resulting in better aircraft deicing fluid performance.

4 CONCLUSIONS

The present study investigated the effect of nano-additives that can help optimize the performance and improve the thermophysical properties of aircraft de/anti-icing fluid. The main results of the current work are summarized below:

(1) The results showed that the thermal conductivity, surface tension, and dynamic viscosity of the hybrid nanofluids are depended on the temperatures and concentrations of the nanoparticles, especially at temperatures below freezing.

(2) The thermal conductivity results of graphene TiO2/aircraft deicing fluid/water hybrid nanofluid show that the thermal conductivity properties and thus the efficiency of the aircraft deicing fluid are improved by the addition of nanoparticles. It was found that the largest improvement in thermal conductivity of the hybrid nanofluid is 41.93%, which is achieved at a volume fraction of nanoparticles of 2.5% at temperature of 303.15 K.

(3) The surface tension of the hybrid nanofluid decreases with increasing temperature. The surface tension improves by 43.61%, 39.77%, and 51.98% at a concentration of 2.5%, 2%, and 2% by volume at temperatures of 258.15 K, 268.15 K, and 283.15 K, respectively. Considering the performance of the aircraft deicing fluid, the increase in the surface tension of the fluid helps to improve its performance in covering the aircraft surfaces against the precipitation of supercooled raindrops and snow, resulting in better performance of the aircraft deicing fluid.

(4) Hybrid nanofluids exhibit surprising rheological behaviour at subfreezing temperatures and low concentrations, possibly due to oleic acid and graphene nanoplatelets.

(5) Experiments have shown that the inclusion of nanoparticles in the base fluid significantly increases viscosity. Based on the results of dynamic viscosity measurement, the addition of nanoparticles in the volume fraction ranges from 0 to 0.5%, in addition to increasing the viscosity, shows non-Newtonian behavior Shear-thinning nanofluid the base, which is the main requirement for the performance of the aircraft de / anti-icing fluid. Therefore, the addition of these two types of nanoparticles in volume fractions below 0.5% helps to improve the performance of aircraft de-icing fluid.

REFERENCES

[1] Yu, W., Xie, H., A Review on Nanofluids: Preparation, Stability Mechanisms, and Applications, Journal of Nanomaterials, Vol. 2012, 2012, DOI: 10.1155/2012/435873.

[2] Sundar, L. S., Sharma, K. V., Singh, M. K., and Sousa, A. C. M., Hybrid Nanofluids Preparation, Thermal Properties, Heat Transfer and Friction Factor–a Review, Renewable and Sustainable Energy Reviews, Vol. 68, No. 2016, 2017, pp. 185–198, DOI: 10.1016/j.rser.2016.09.108.

[3] Patra, A. K., Nayak, M. K., and Misra, A., Viscosity of Nanofluids-A Review, Int. J. of Thermofluid Science and Technology, Vol. 7, No. 2, 2020, pp. 070202, DOI: 10.36963/ijtst.2020070202.

[4] Sajid, M.U., Ali, H. M., Thermal Conductivity of Hybrid Nanofluids: A Critical Review, International Journal of Heat and Mass Transfer, Vol. 126, 2018, pp. 211–234, DOI: 10.1016/j.ijheatmasstransfer.2018.05.021.

[5] Sarkar, J., Ghosh, P., and Adil, A., A Review on Hybrid Nanofluids: Recent Research, Development and Applications, Renewable and Sustainable Energy Reviews, Vol. 43, 2015, pp. 164–177, DOI: 10.1016/j.rser.2014.11.023.

[6] Nayebpashaee, N., Hadavi, S. M. M., Thermal Conductivity and Rheological Studies for Graphene-Al2O3/Ethylene Glycol-Water Hybrid Nanofluid at Low Temperatures, Vol. 73, 2022, pp. 139–160, DOI: 10.4028/p-h9do2u, Trans Tech Publications Ltd.

[7] Jan, A., Mir, B., and Mir, A. A., Hybrid Nanofluids: An Overview of Their Synthesis and Thermophysical Properties, arXiv, No. 3, 2019.

[8] Boroomandpour, A., Toghraie, D., and Hashemian, M. A., Comprehensive Experimental Investigation of Thermal Conductivity of a Ternary Hybrid Nanofluid Containing MWCNTs-Titania-Zinc Oxide/Water-Ethylene Glycol (80: 20) as Well As Binary and Mono Nanofluids, Synthetic Metals, Vol. 268, No. July, pp. 116501, 2020, DOI: 10.1016/j.synthmet.2020.116501.

[9] Alarifi, I. M., Alkouh, A. B., Ali, V., Nguyen, H. M., and Asadi, A., On the Rheological Properties of MWCNT-TiO2/oil Hybrid Nanofluid: An Experimental Investigation on The Effects of Shear Rate, Temperature, And Solid Concentration of Nanoparticles, Powder Technology, Vol. 355, pp. 157–162, 2019, DOI: 10.1016/j.powtec.2019.07.039.

[10] Transport Canada, Guidelines for Aircraft Ground Icing Operations (Chapter 13), 2005, pp. 74.

[11] Federal Aviation Administration, Advisory Circular (AC No. 00-6B), No. January, 2016, pp. 213, DOI: AFS-800 AC 91-97.

[12] Thomas, S. K., Cassoni, R. P., and MacArthur, C. D., Aircraft Anti-Icing and De-Icing Techniques and Modeling, Journal of Aircraft, Vol. 33, No. 5, 1996, pp. 841–854, DOI: 10.2514/3.47027.

[13] Riley, J., Underwood, W., and Pugacz, E., The FAA Ground Icing Research Program, In45th AIAA Aerospace Sciences Meeting and Exhibit 2007 Jan 8 (pp. 694), Vol. 12, No. January, 2007, pp. 8575–8591.

[14] ICAO, Manual of Aircraft Ground De-Icing / Anti-Icing Operations, 2000, pp. 1.

[15] Goraj, Z., An Overview of The Deicing and Anti-Icing Technologies with Prospects for The Future, In 24th International Congress of The Aeronautical Sciences, 29 August - 3 Sept., 2004, pp. 1–11.

[16] Aminian, E., Ahmadi, B., Numerical Investigation on Heat Transfer and Performance Number of Nanofluid Flow inside a Double Pipe Heat Exchanger Filled with Porous Media, International Journal of Advanced Design & Manufacturing Technology (ADMT Journal), Vol. 11, No. 4, 2018, pp. 31–46.

[17] Apmann, K., Fulmer, R., Soto, A., and Vafaei, S., Thermal Conductivity and Viscosity: Review and Optimization of Effects of Nanoparticles, Materials,

Vol. 14, No. 5, 2021, pp. 1–75, DOI: 10.3390/ma14051291.
[18] Nourbakhsh, A., Sadeghi, A. R., Numerical Study of the Flow Field and Heat Transfer of a Non-Newtonian Magnetic Nanofluid in A Vertical Channel Affected by A Magnetic Field. International Journal of Advanced Design & Manufacturing Technology (ADMT Journal), Vol. 15, No. 2, 2022, pp. 105-118, DOI: 10.30495/admt.2022.1939334.1312.Biographical.
[19] Nayebpashaee, N., Hadavi, S. M. M., Thermal Conductivity and Surface Tension of Graphene–Al2O3/Ethylene Glycol–Water Hybrid Nanofluid at Sub-Zero Temperatures: An Experimental Study. Journal of Thermal Analysis and Calorimetry, No. 0123456789, 2022, pp. 13–15, 2022, DOI: 10.1007/s10973-022-11587-y.
[20] Talebi, M., Tabibian, M., Magnetic Field Effect on Ferro-Nanofluid Heat Transfer in a Shell and Tube Heat Exchanger with Seven Twisted Oval Tubes, International Journal of Advanced Design & Manufacturing Technology (ADMT Journal), Vol. 15, No. 2, 2022, pp. 39–48, DOI:10.30495/admt.2022.1937049.1300.
[21] Davoudi, A., Daneshmand, S., Monfared, V., and Mohammadzadeh, K., Numerical Simulation on Heat Transfer of Nanofluid in Conical Spiral Heat Exchanger, Progress in Computational Fluid Dynamics, an International Journal, Vol. 21, No. 1, 2021, pp. 52-63, DOI: 10.1504/PCFD.2021.112620.
[22] Bozorgan, N., Shafahi, M., Evaluation of γ-Al2O3/n-decane Nanofluid Performance in Shell and Tube Heat Recovery Exchanger in a Biomass Heating Plant. International Journal of Advanced Design & Manufacturing Technology (ADMT Journal), Vol. 9, No. 2, 2016, pp. 69-77.
[23] Malekzadeh, A., Pouranfard, A. R., Hatami, N., Kazemnejad Banari, A., and Rahimi, M. R., Experimental Investigations on The Viscosity of Magnetic Nanofluids Under the Influence of Temperature, Volume Fractions of Nanoparticles and External Magnetic Field, Journal of Applied Fluid Mechanics, Vol. 9, No. 2, 2016, pp. 693–697, DOI: 10.18869/acadpub.jafm.68.225.24022.
[24] Najafi, M., Najafi, M., Experimental and Analytical Study of Aluminum-oxide Nanofluid Implication for Cooling System of an Amphibious Engine, International Journal of Advanced Design & Manufacturing Technology (ADMT Journal), Vol. 10, No. 1, 2017, pp. 51-56.
[25] Demirkır, Ç., Ertürk, H., Rheological and Thermal Characterization of Graphene-Water Nanofluids: Hysteresis Phenomenon, International Journal of Heat and Mass Transfer, Vol. 149, 2020, pp. 3–11, DOI: 10.1016/j.ijheatmasstransfer.2019.119113.
[26] Rahmati, A., Azizi, T., Mousavi, S., and Zarareh, A., Effects of Slip Boundaries on Mixed Convection of Al2O3-Water Nanofluid in Microcavity, International Journal of Advanced Design & Manufacturing Technology (ADMT Journal), Vol. 8, No. 2, 2015, pp. 47-54.
[27] Kazemi, I., Sefid, M., and Afrand, M., A Novel Comparative Experimental Study on Rheological Behavior of Mono & Hybrid Nanofluids Concerned Graphene and Silica Nano-Powders: Characterization, Stability and Viscosity Measurements, Powder Technology, Vol. 366, 2020, pp. 216–229, DOI: 10.1016/j.powtec.2020.02.010.
[28] Yu, W., Xie, H., Chen, L., and Li, Y., Investigation of Thermal Conductivity and Viscosity of Ethylene Glycol Based ZnO Nanofluid, Thermochimica Acta, Vol. 491, No. 1–2, 2009, pp. 92–96, DOI: 10.1016/j.tca.2009.03.007.
[29] Banisharif, A., Aghajani, M., Van Vaerenbergh, S., Estellé, P., and Rashidi, A., Thermophysical Properties of Water Ethylene Glycol (WEG) mixture-based Fe3O4 nanofluids at low Concentration and Temperature, Journal of Molecular Liquids, Vol. 302, 2020, pp. 112606, DOI: 10.1016/j.molliq.2020.112606.
[30] Standard, SAE Aerospace, Standard Test Method for Aerodynamic Acceptance of SAE AMS 1424 and SAE AMS 1428 Aircraft Deicing/Anti-icing Fluids, AS5900 Rev. A., 2017.
[31] Kilfrost, Kilfrost ABC-3, No. 1907, 2015.
[32] Salih, N., Salimon, J., and Yousif, E., The Physicochemical and Tribological Properties of Oleic Acid Based Triester Biolubricants, Industrial Crops and Products, Vol. 34, No. 1, 2011, pp. 1089–1096, DOI: 10.1016/j.indcrop.2011.03.025.
[33] Lide, D. R., CRC Handbook of Chemistry and Physics (Vol. 85). ed., 2004. pp. 2313–2314.
[34] Owen, M. S., ASHRAE Handbook: Fundamentals, Vol. 30329, No. 404, 2009.
[35] Sayah, A., Habelhames, F., Bahloul, A., Nessark, B., Bonnassieux, Y., Tendelier, D., and El Jouad, M., Electrochemical Synthesis of Polyaniline-Exfoliated Graphene Composite Films and Their Capacitance Properties, Journal of Electroanalytical Chemistry, Vol. 818, No. April, 2018, pp. 26–34, DOI: 10.1016/j.jelechem.2018.04.016.
[36] Siburian, R., Sihotang, H., Raja, S. L., Supeno, M., and Simanjuntak, C., New Route to Synthesize of Graphene Nano Sheets. Oriental Journal of Chemistry, Vol. 34, No. 1, 2018, pp. 182–187, DOI: 10.13005/ojc/340120.
[37] Shelke, P. D., Rajbhoj, A. S., Nimase, M. S., Tikone, G. A., Zaware, B. H., and Jadhav, S. S., An Efficient, Solvent Free One Pot Synthesis of Tetrasubstitued Imidazoles Catalyzed by Nanocrystalline Γ-Alumina, Orient. J. Chem., Vol. 32, No. 4, 2016, pp. 2007–2014, DOI: 10.13005/ojc/320427.
[38] Sifontes, Á. B., et al., Preparation of Functionalized Porous Nano-γ-Al2O3 Powders Employing Colophony Extract, Biotechnol. Reports, Vol. 4, No. 1, 2014, pp. 21–29, DOI: 10.1016/j.btre.2014.07.001.
[39] Khodadadi Darban, A., Kianinia, Y., and Taheri-Nassaj, E., Synthesis of Nano-Alumina Powder from Impure Kaolin and Its Application for Arsenite Removal from Aqueous Solutions, Journal of Environmental Health Science and Engineering, Vol. 11, No. 1, 2013, pp. 1-11, DOI: 10.1186/2052-336x-11-19.
[40] Rubbi, F., Das, L., Habib, K., Aslfattahi, N., Saidur, R., and Rahman, M. T., State-Of-The-Art Review on Water-Based Nanofluids for Low Temperature Solar Thermal Collector Application, Solar Energy Materials and Solar Cells, Vol. 230, 2021, pp. 111220, DOI: 10.1016/J.SOLMAT.2021.111220.

[41] Xian, H. W., Sidik, N. A., and Saidur, R., Impact of Different Surfactants and Ultrasonication Time on The Stability and Thermophysical Properties of Hybrid Nanofluids. International Communications in Heat and Mass Transfer, Vol. 110, 2020, pp.104389, DOI: 10.1016/j.icheatmasstransfer.2019.104389.

[42] Rubbi, F., Habib, K., Saidur, R., Aslfattahi, N., Yahya, S. M., and Das, L., Performance Optimization of a Hybrid PV/T Solar System Using Soybean Oil/MXene Nanofluids as A New Class of Heat Transfer Fluids, Solar Energy, Vol. 208, No. July, pp. 124–138, 2020, DOI: 10.1016/j.solener.2020.07.060.

[43] Kulkarni, D. P., Das, D. K., and Chukwu, G. A., Temperature Dependent Rheological Property of Copper Oxide Nanoparticles Suspension (Nanofluid), Journal of Nanoscience and Nanotechnology, Vol. 6, No. 4, 2006, pp. 1150–1154, DOI: 10.1166/jnn.2006.187.

[44] Sha, X., Yu, K., Cao, H., and Qian, K., Shear Thickening Behavior of Nanoparticle Suspensions with Carbon Nanofillers, Journal of Nanoparticle Research, Vol. 15, No. 7, 2013, pp. 1-11, DOI: 10.1007/s11051-013-1816-x.

[45] Mahbubul, I. M., Saidur, R., and Amalina, M. A., Latest Developments on The Viscosity of Nanofluids, International Journal of Heat and Mass Transfer, Vol. 55, No. 4, 2012, pp. 874–885, DOI: 10.1016/j.ijheatmasstransfer.2011.10.021.

[46] Zhao, N., Li, Z., Experiment and Artificial Neural Network Prediction of Thermal Conductivity and Viscosity for Alumina-Water Nanofluids, Materials, Vol. 10, No. 5, 2017, pp. 552, DOI: 10.3390/ma10050552.

[47] Chen, H., Ding, Y., and Tan, C., Rheological Behaviour of Nanofluids, New Journal of Physics, Vol. 9, 2007, pp. 367, DOI: 10.1088/1367-2630/9/10/367.

[48] Lenin, R., Joy, P. A., and Bera, C., A Review of The Recent Progress on Thermal Conductivity of Nanofluid, Journal of Molecular Liquids, Vol. 338, 2021, pp. 116929, DOI: 10.1016/j.molliq.2021.116929.

[49] Bhuiyan, M. H., Saidur, R., Amalina, M. A., Mostafizur, R. M., and Islam, A. K., Effect of Nanoparticles Concentration and Their Sizes on Surface Tension of Nanofluids, Procedia Engineering, Vol. 105, No. Icte 2014, pp. 431–437, 2015, DOI: 10.1016/j.proeng.2015.05.030.

[50] Tanvir, S., Qiao, L., Surface Tension of Nanofluid-Type Fuels Containing Suspended Nanomaterials, Nanoscale Research Letters, Vol. 7, No.1, 2012, pp. 1-10, DOI: 10.1186/1556-276X-7-226.

[51] Zhu, D. S., Wu, S. Y., and Wang, N., Surface Tension and Viscosity of Aluminum Oxide Nanofluids, In AIP (American Institute of Physics Conference Proceedings) Mar 1, Vol. 1207, No. 1, 2010, pp. 460-464, DOI: 10.1063/1.3366409.